Cell Metabolism, Volume *30*

Supplemental Information

Age Mosaicism across Multiple Scales in Adult Tissues

Rafael Arrojo e Drigo, Varda Lev-Ram, Swati Tyagi, Ranjan Ramachandra, Thomas Deerinck, Eric Bushong, Sebastien Phan, Victoria Orphan, Claude Lechene, Mark H. Ellisman, and Martin W. Hetzer

Supplementary Figure 1

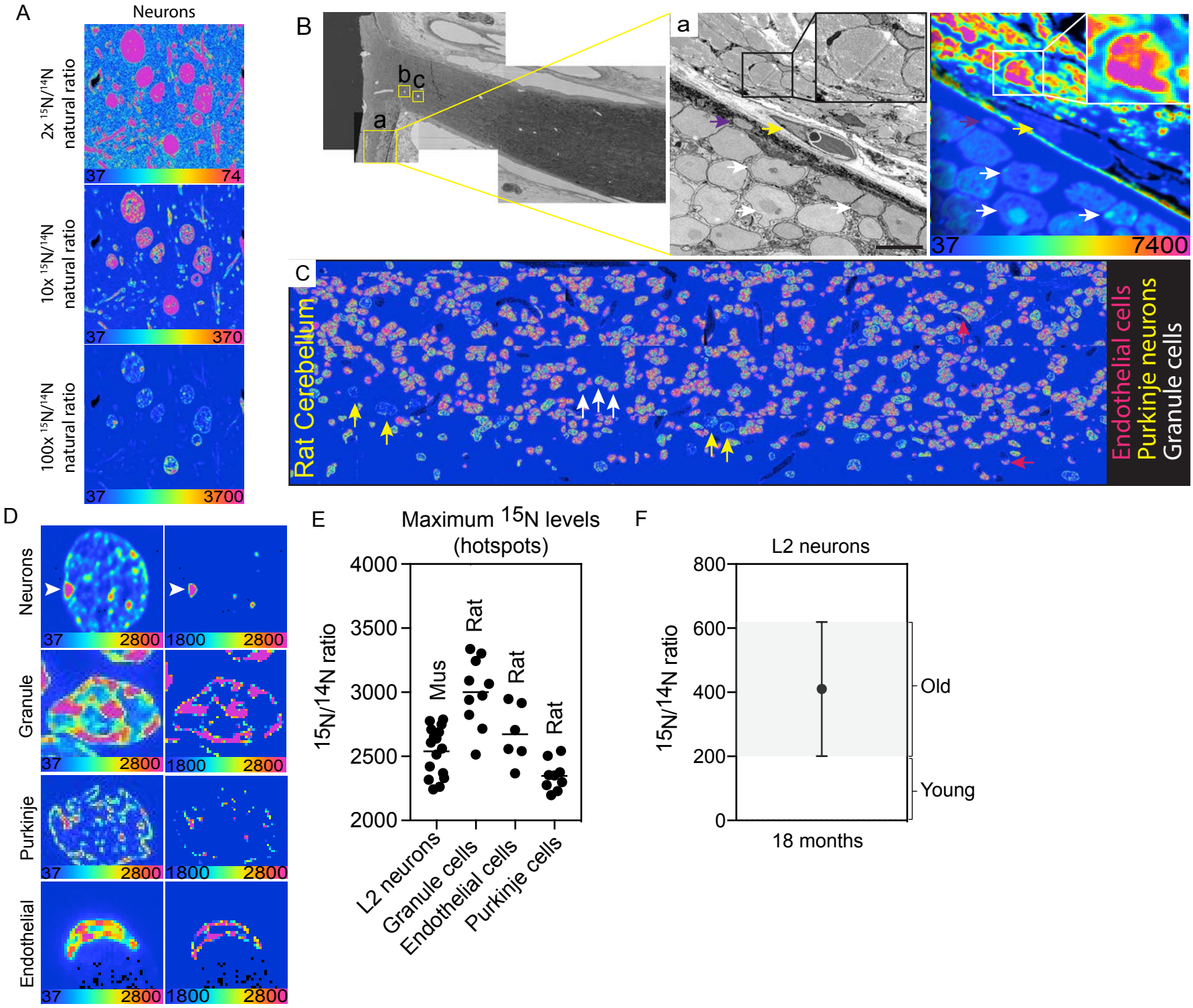

Supplementary Figure 2

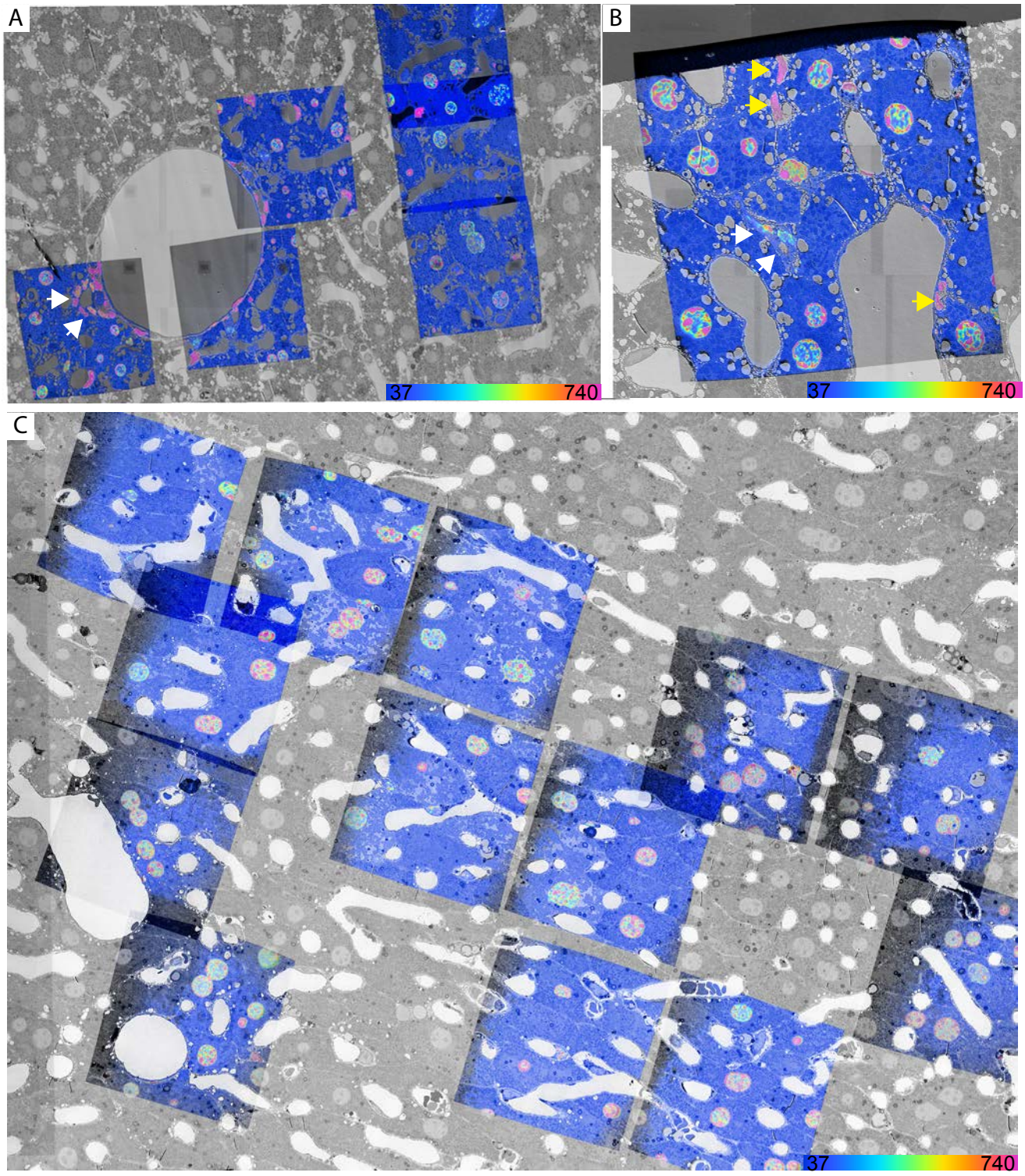

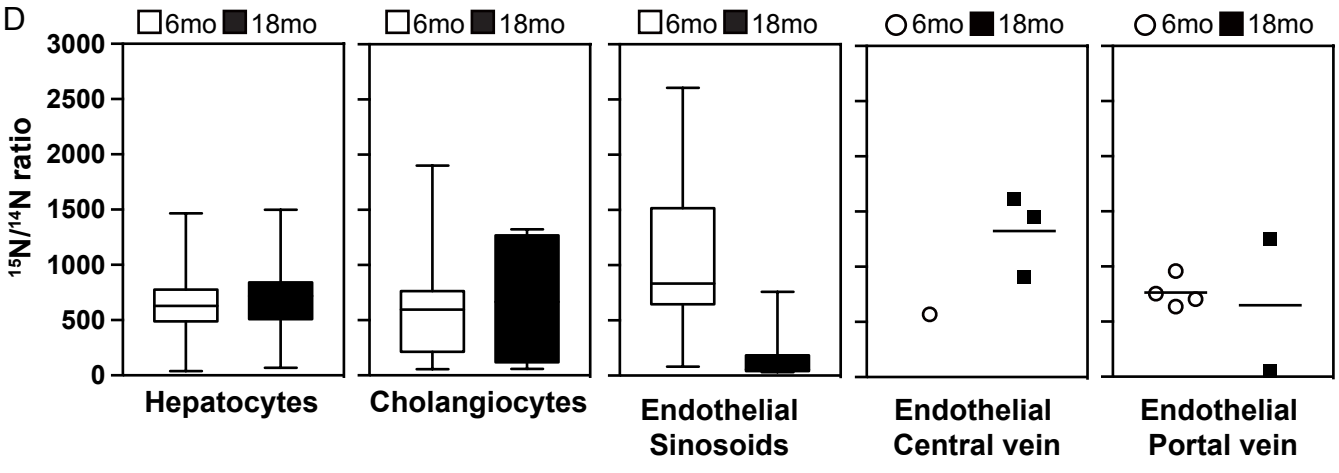

Supplementary Figure 3

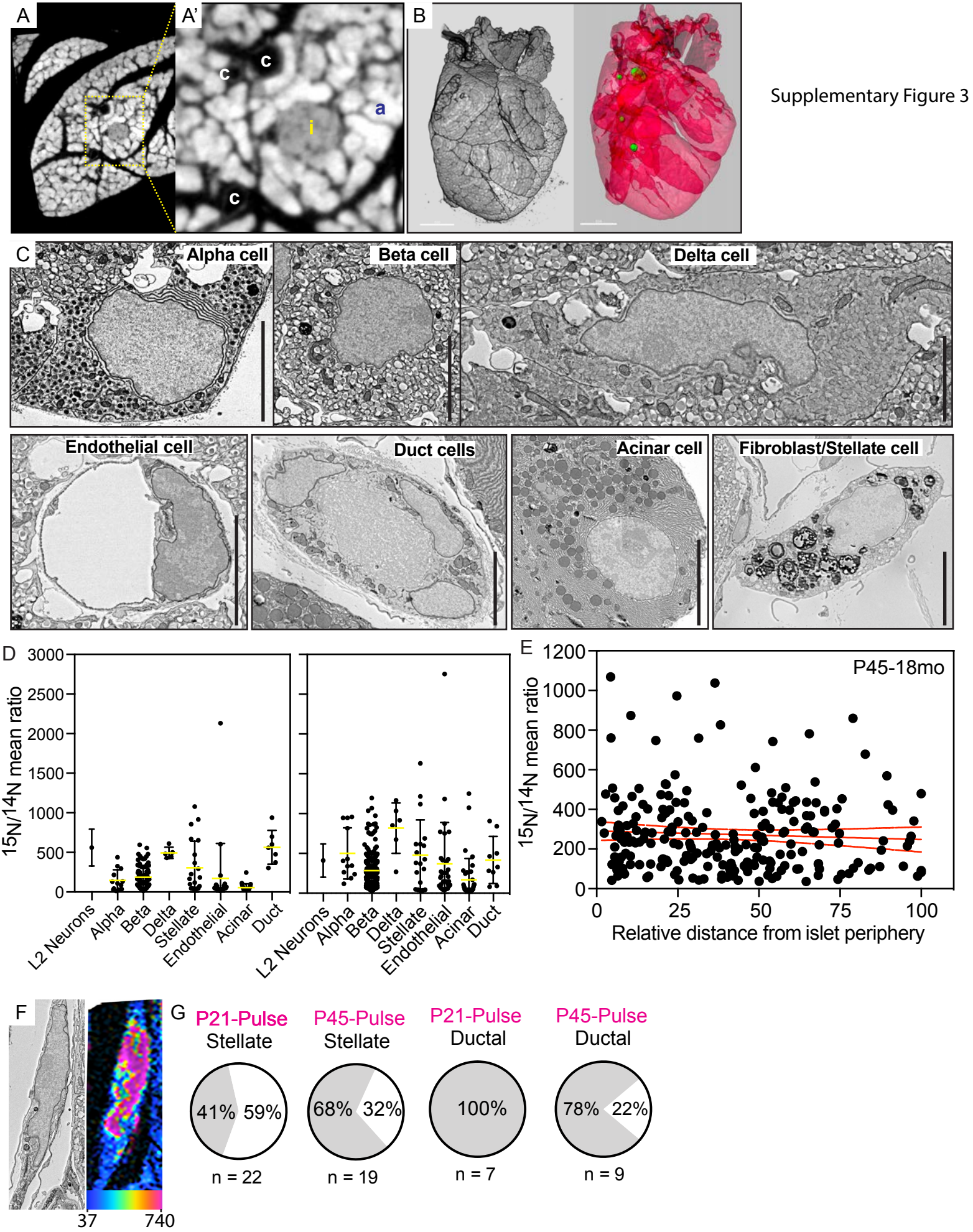

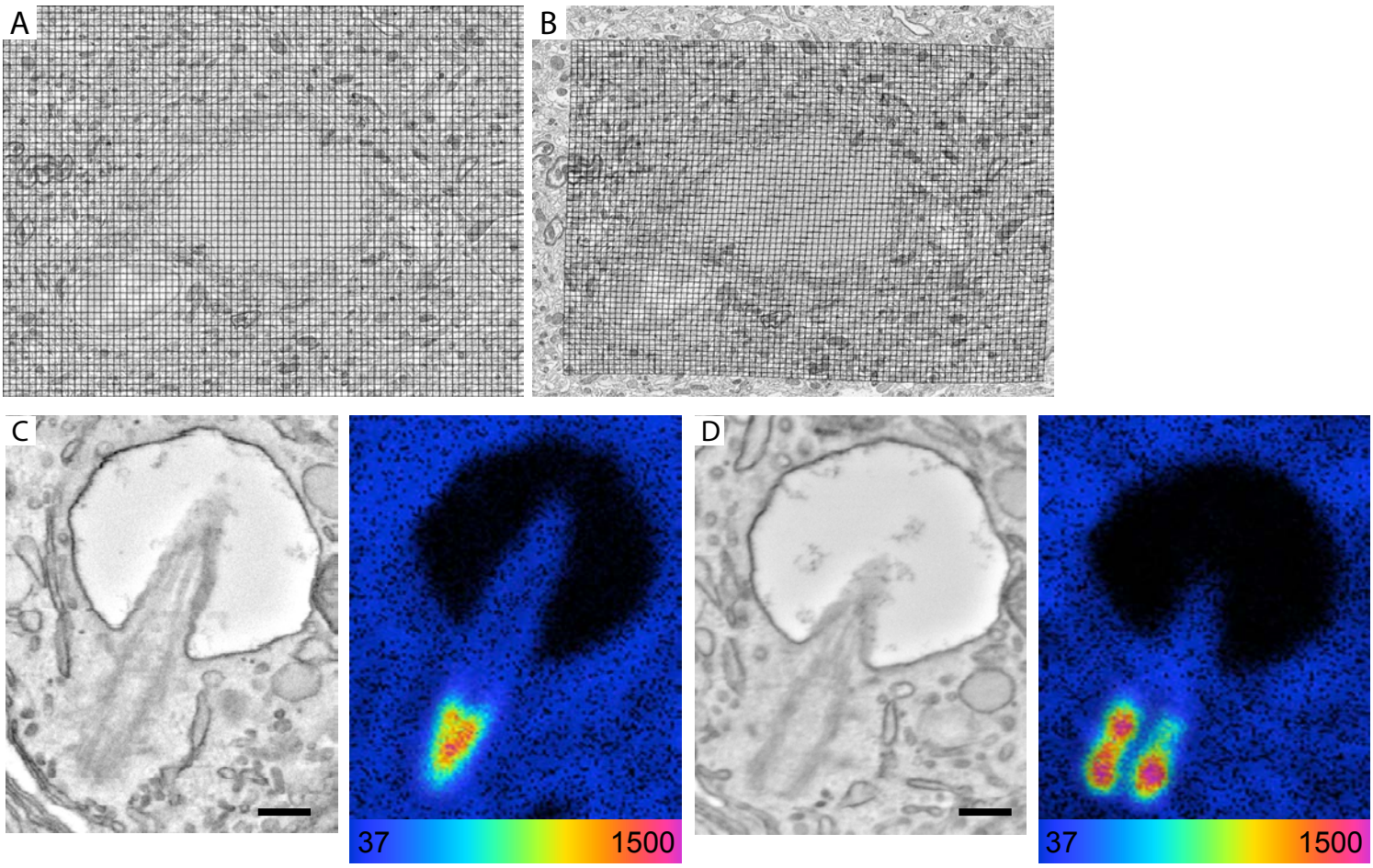

Supplementary Figure 4

Figure S1 – Related to Figure 1. (A) Three panels showing the $^{15}N/^{14}N$ ratio generated after MIMS mapping of a P45-SILAM mouse L2 cortex after 6-months of chase. The images are shown using the HSI scaled to display pixels with intensities 2, 10 or 100x higher than the natural ratio. **(B)** Large field of view scanning electron microscopy (SEM) of a 6-month chase mouse optic nerve head (ONH) longitudinal section. Yellow square insets: (a) EM-MIMS imaging of a portion of the retina. Left corner, cells in the inner nuclear layer (INL) are indicated by white arrowheads. Following the INL, the darker retinal pigment epithelium (RPE) can be seen and where a hexagonal cell nucleus is indicated by the purple arrowhead. To the right of the RPE, extra cellular matrix (ECM) fiber bundles from the Brunch membrane (BrM) are seen. The yellow arrowhead indicates the nucleus of an endothelial cell that is part of a capillary vessel located between the BrM and the ECM-rich choroid region (inset of (a)). Insets (b-c) indicate the position of two different capillaries imaged with MIMS-EM and the data is shown in detail in Figure1 panels C-F. **(C)** Multi-tile MIMS imaging of a large cross-section of the granular cell layer of a 6-month chase rat cerebellum. Yellow arrowheads point to examples of Purkinje neuron nuclei, while white arrowheads indicate granule cells nuclei and pink arrowheads show the position of capillary endothelial cell nuclei. **(D)** Ratiometric $^{15}N/^{14}N$ $x10^4$ maps are shown with the full range (37 to 2800) (left) or with $^{15}N/^{14}N$ signal thresholds applied (right, 1800 to 2800) to highlight ^{15}N hotspots (indicated by white arrowheads on top row as an example). **(E)** Quantification of the $^{15}N/^{14}N$ ratio in the intra-nuclear regions (n=4-6 hotspots per cell type) containing the highest levels of ^{15}N isotope in mouse L2 neurons, rat cerebellar granule cells, Purkinje cells or endothelial cells. **(F)** $^{15}N/^{14}N$ ratio in the nucleus of L2 neurons. To classify cells as old or young cells, we first determined the range of $^{15}N/^{14}N$ observed in cortical neurons (n = 60 neuron nuclei, highlighted in light gray shade). Next, any given cell was determined to be “old” if its mean nuclear $^{15}N/^{14}N$ was within the observed range in neurons. However, if the mean $^{15}N/^{14}N$ of any given cell was below this range in neurons, that cell was classified as “young”. The MIMS images are shown as $^{15}N/^{14}N$ $x10^4$ and scaled with a hue saturation intensity (HSI). In (a), Scale bar 5um. Data in (F) is shown as $\pm$ standard deviation of the mean.

Figure S2 – Related to Figure 2. (A) Large field of view of a SEM micrograph overlaid with a $^{15}N/^{14}N$ ratio MIMS image of a hepatic lobule from a mouse labelled with ^{15}N-SILAM until P45 chased for 6-months (P45-6mo). A cross section of a biliary duct is shown where nucleated cholangiocytes are visible (indicated by the white arrowheads). **(B)** Close view of perivascular region of the liver from the mouse P45-6mo. Yellow arrowheads indicate the overlap of ^{15}N-rich signal with bundles of collagen fibers (ECM matrix). White arrowheads indicate the location of two cholangiocytes forming a partially collapsed biliary duct. **(C)** Same as (A), but from a mouse labelled with ^{15}N-SILAM until P45 chased for 18-months (P45-18mo). **(D)** Quantification of $^{15}N/^{14}N$ ratio from hepatocytes, cholangiocytes, hepatic stellate-like cells, and endothelial cells in portal and central veins, and in sinusoids. Data is shown in box whiskers with median, maximum and minimum range shown. Data is from n=126 (P45-6mo) and n=154 (P45-18mo) hepatocytes, n=29 (P45-6mo) and n=6 (P45-18mo) cholangiocytes, n=36 (P45-6mo) and n=16 (P45-18mo) stellate-like cells, n=23 (P45-6mo) and n=18 (P45-18mo) sinusoid endothelial cells, n=1 (P45-6mo) and n=3 central vein endothelial cells, n=4 (P45-6mo) and n=2 (P45-18mo) portal vein endothelial cells. At the bottom of the MIMS images, the heat map shows the indicated $^{15}N/^{14}N$ $x10^4$ as a hue saturation intensity (HSI).

Figure S3 – Related to Figure 3. (A) Cross-section image of a mouse pancreas acquired using XRM imaging. Yellow-dotted square indicates the position of an islet of Langerhans. Inset of (A) shows a magnified view of the islet (i). Capillaries (c) are seen on the top and bottom left corners of the image. Acinar tissue (a) is seen surrounding the islet. **(B)** Three-dimensional (3D) reconstruction of a small mouse pancreas tissue block acquired with XRM. In grey, complete volume of the pancreas block is shown. In red, the 3D pancreas volume was made partially

transparent and the location of endogenous islets are shown in green and their respective volumes are listed to the right of the image. **(C)** Representative images of alpha, beta, delta, endothelial, duct, acinar and fibroblasts/pancreatic stellate cells scanned SEM. **(D)** Plot of nuclear $^{15}N/^{14}N$ ratios of pancreatic cells in from mice labelled with ^{15}N-SILAM until P45 or P21 and chased for 18- and 26-months (P45-18mo and P21-26mo, respectively). Islet data is shown as ± standard deviation of the mean for different cell type and individual levels for each cell are shown as dots. The neuronal mean and standard deviation for each respective animal is shown as well. Data acquired from n=3 islets for P45-18mo and n=4 islets for P45-26mo. **(E)** Relationship between the $^{15}N/^{14}N$ ratio of old and young beta cells and relative their distance to the islet periphery of a mouse labelled with ^{15}N-SILAM until P45 chased for 18-months (P45-18mo). Red lines indicate the mean and confidence intervals of a linear regression test ($r^2<0.005$). Each point represents individual beta cells (n=228, from n=3 islets). **(F)** SEM and MIMS of a pancreatic stellate cell located in the periphery of an islet of Langerhans from the P45-18mo mouse. **(G)** Relative turnover, in percentages, of stellate or ductal cells that are as old (grey) or younger (white) than L2 neurons from ^{15}N-SILAM P21 mouse chased for 26 months or from the ^{15}N-SILAM P45 mouse chased for 18 months. The total number of cells analyzed for each cell type is listed underneath each pie chart. At the bottom of the MIMS images, the heat map shows the $^{15}N/^{14}N$ $x10^4$ and scaled with a hue saturation intensity (HSI). Scale bars: (B), 500um; (C), 5um.

Figure S4 – Related to Figure 4. (A) Representative image of a SEM micrograph of the neuron imaged with MIMS-EM shown in (Figure4D). The SEM image has been overlaid with a grid that represents the re-sized MIMS image before processing (details in the methods section). **(B)** Same as (A), but the grid shows the result of the post-acquisition processing to align the MIMS image on the SEM micrograph. **(C-D)** Two serial sections of a beta cell BB from a P45-^{15}N-SILAM chased for 18 months and imaged with SEM (left panel) and MIMS (right panel). Scale bar, (C-D) 200nm.